Energy Materials

Supplementary Material

Defect-induced-reduced Au quantum dots@MXene decorated separator enables lithium-sulfur batteries with high sulfur utilization

Yahao Du, Yuhong Liu, Feifei Cao*, Huan Ye*

College of Chemistry, Huazhong Agricultural University, Wuhan 430070, Hubei, China.

***Correspondence to:** Prof. Huan Ye, College of Chemistry, Huazhong Agricultural University, No. 1, Shizishan Street, Wuhan 430070, Hubei, China. E-mail: yehuan@mail.hzau.edu.cn; Prof. Feifei Cao, College of Chemistry, Huazhong Agricultural University, No. 1, Shizishan Street, Wuhan 430070, Hubei, China. E-mail: caofeifei@mail.hzau.edu.cn

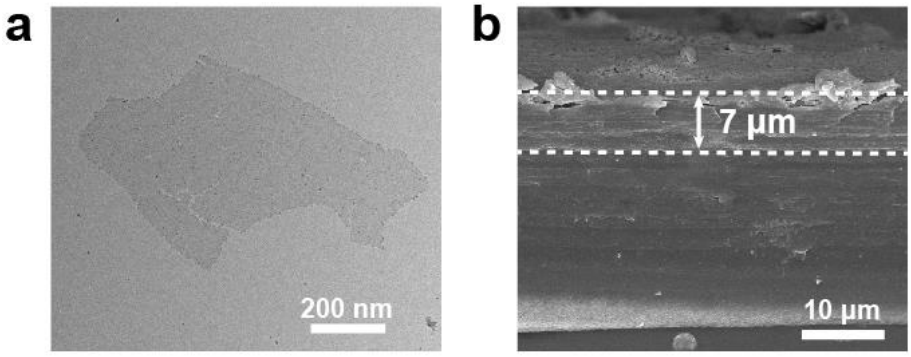

Figure S1. (a) TEM image of MXene nanosheet. (b) Cross-section SEM image of MXene-decorated separator.

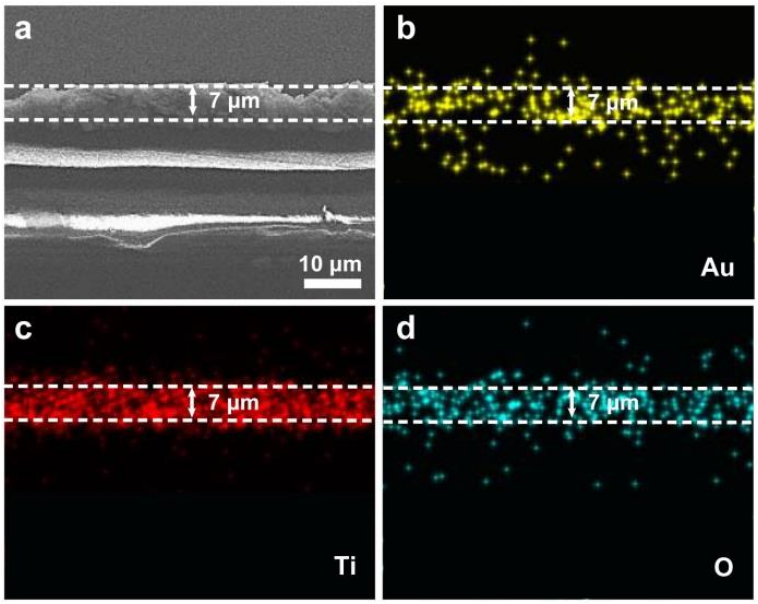

Figure S2. (a) Cross-section SEM image and (b-d) EDX elemental mapping of Au QDs@MXene-decorated separator.

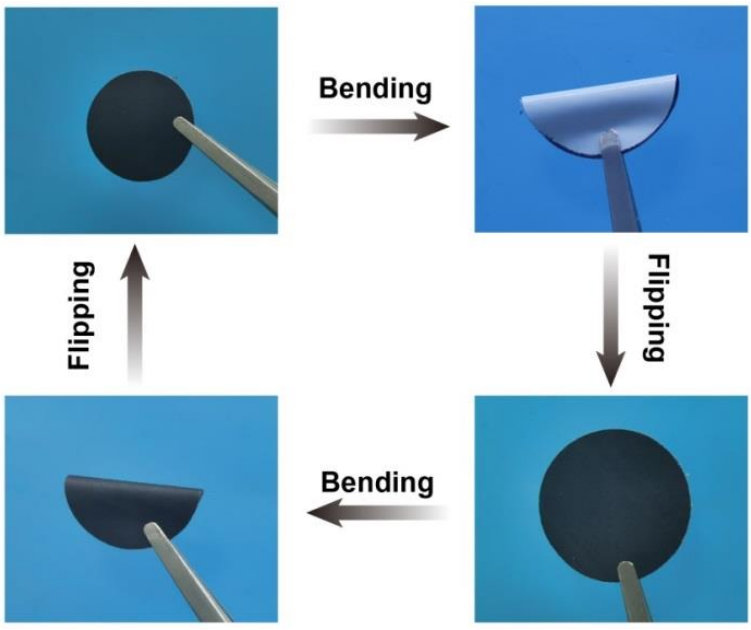

Figure S3. Bending test of Au QDs@MXene-decorated separator.

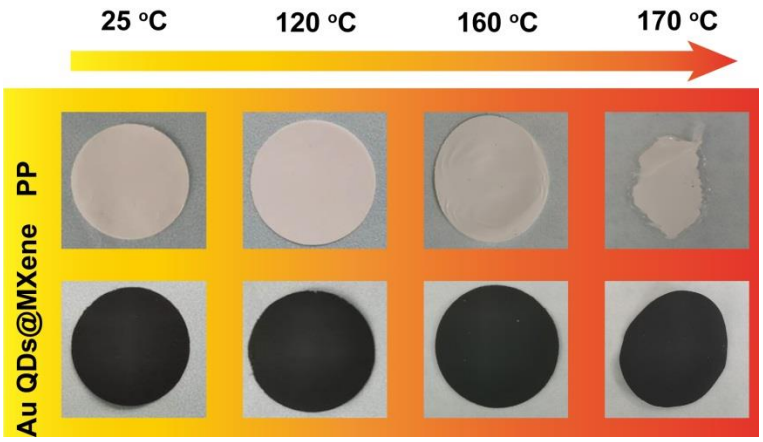

Figure S4. Digital photos of the PP separator and Au QDs@MXene-decorated separator after heating at different temperatures for 30 min.

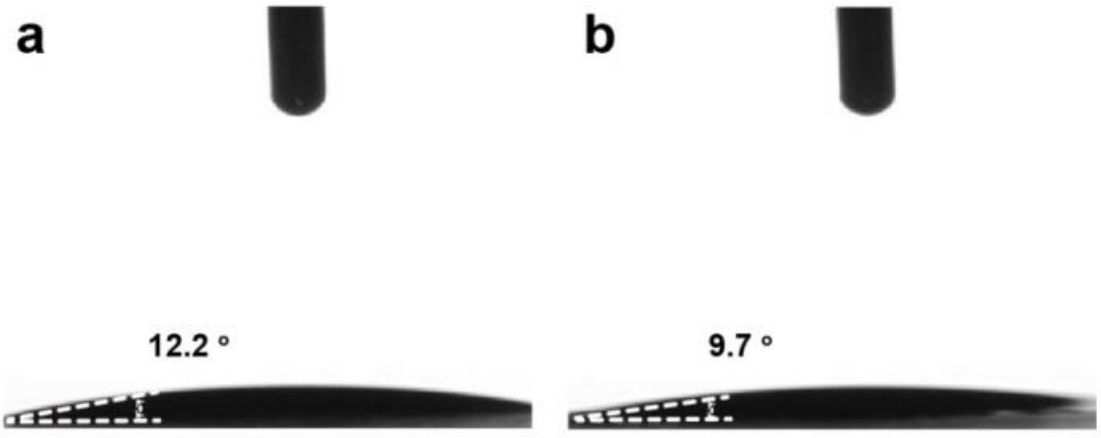

Figure S5. The contact angles between electrolyte and (a) MXene-decorated, (b) Au QDs@MXene-decorated separators.

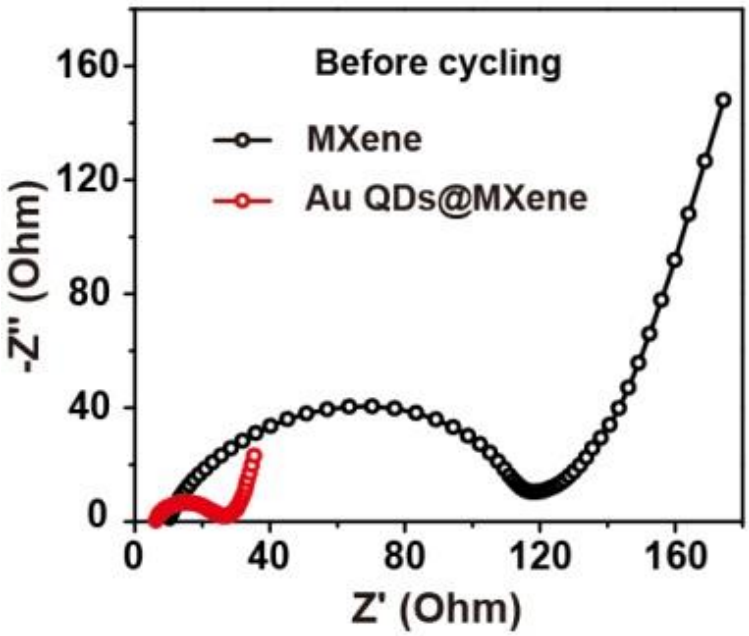

Figure S6. EIS profiles of Li-S cells with MXene-decorated and Au QDs@MXene-decorated separators before cycling.

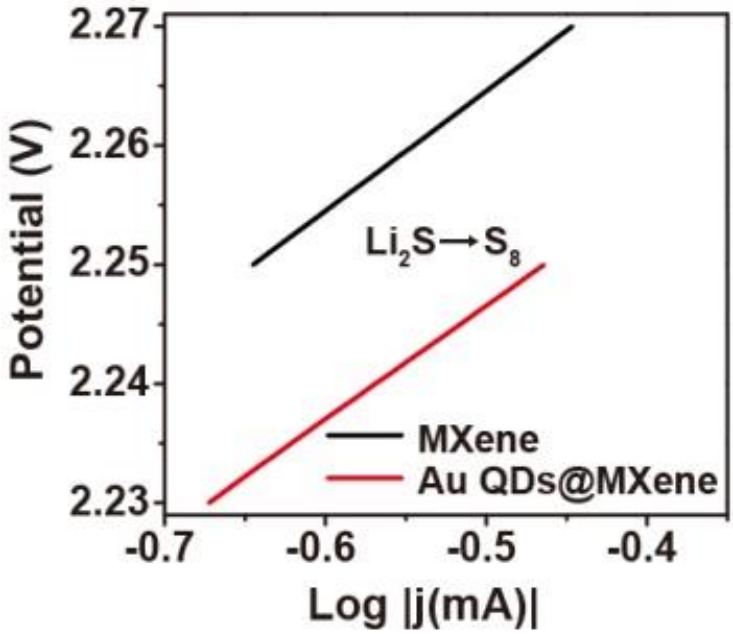

Figure S7. Tafel plots corresponding to the oxidation from Li_2S to S_8.

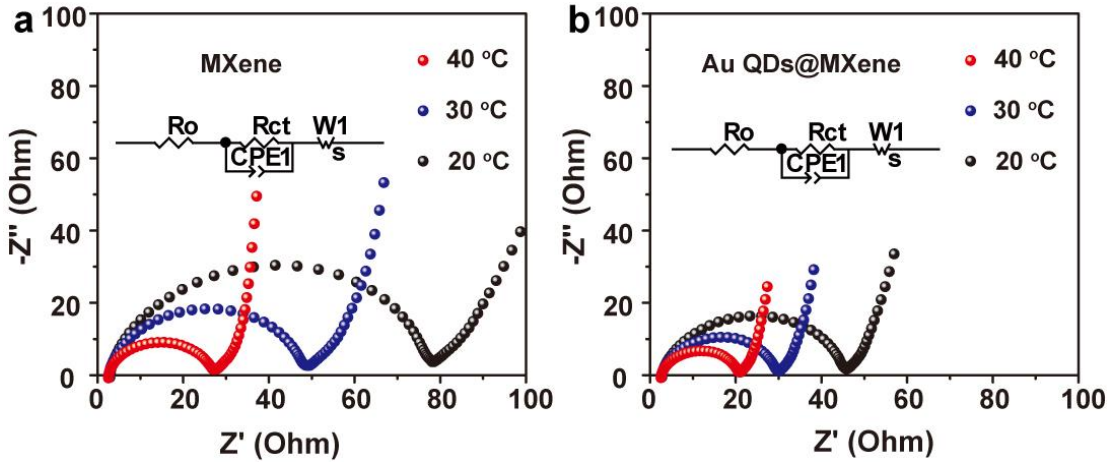

Figure S8. (a,b) EIS profiles of Li-S cells with MXene-decorated and Au QDs@MXene-decorated separators at different temperatures.

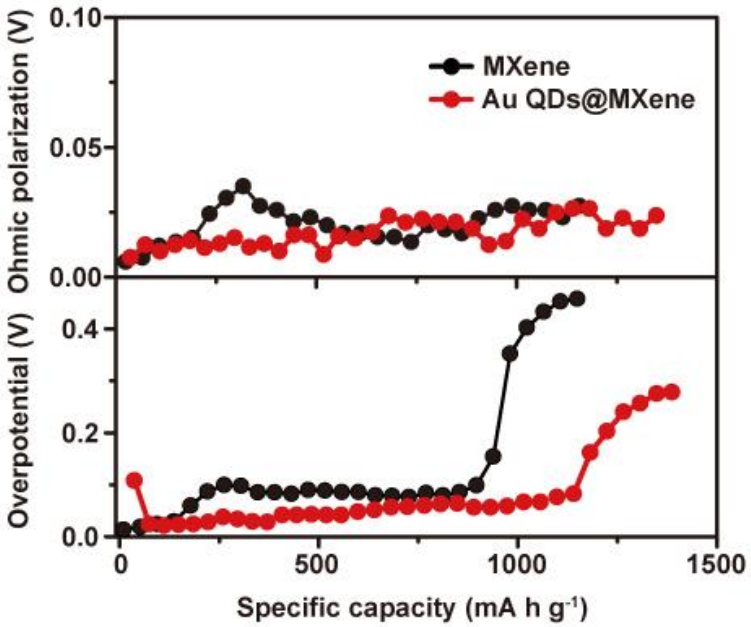

Figure S9. GITT curves of Li-S cells with MXene-decorated and Au QDs@MXene-decorated separators.

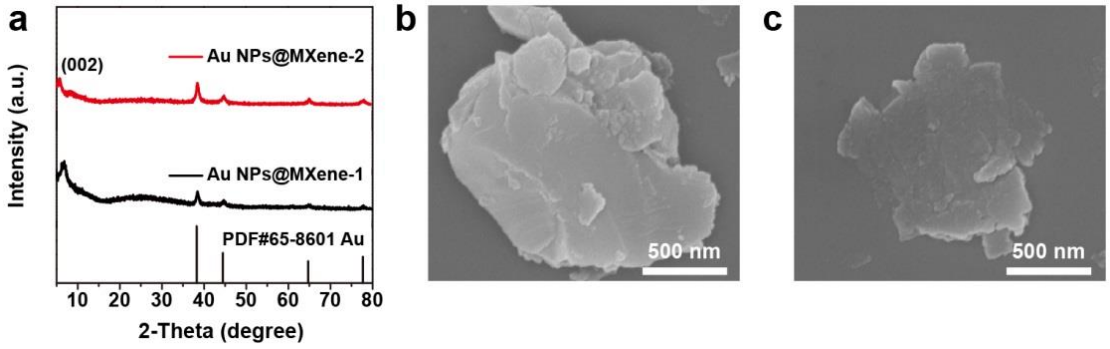

Figure S10. (a) XRD patterns of Au NPs@MXene-1 and Au NPs@MXene-2 heterostructure. (b,c) SEM images of Au NPs@MXene-1 and Au NPs@MXene-2 heterostructure.

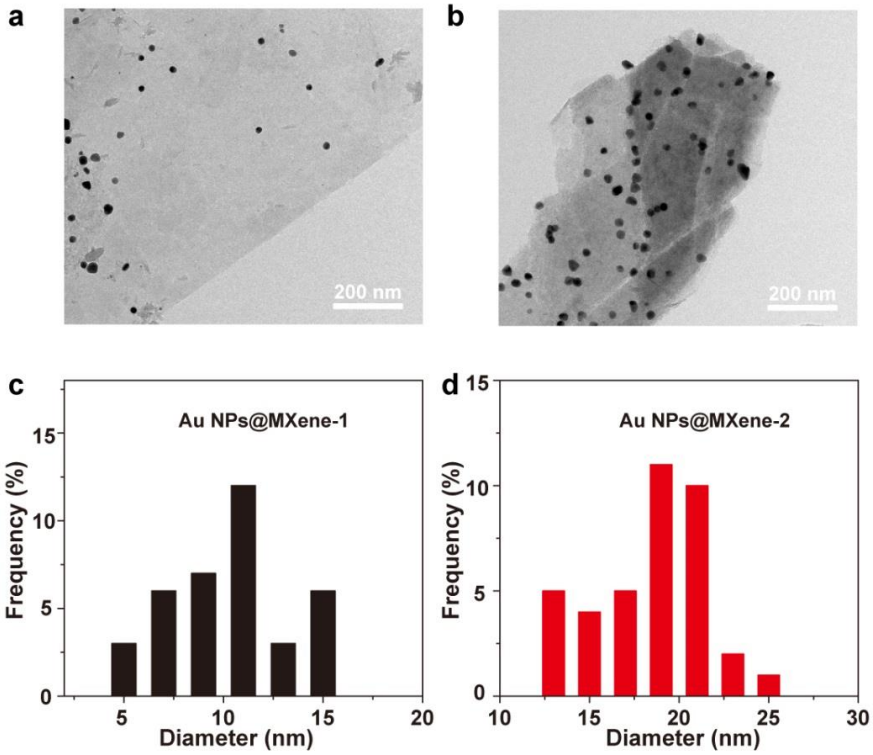

Figure S11. (a,b) HRTEM images of Au NPs@MXene-1 and Au NPs@MXene-2 heterostructure. (c,d) Grain size distribution of Au NPs@MXene-1 and Au NPs@MXene-2 heterostructure.

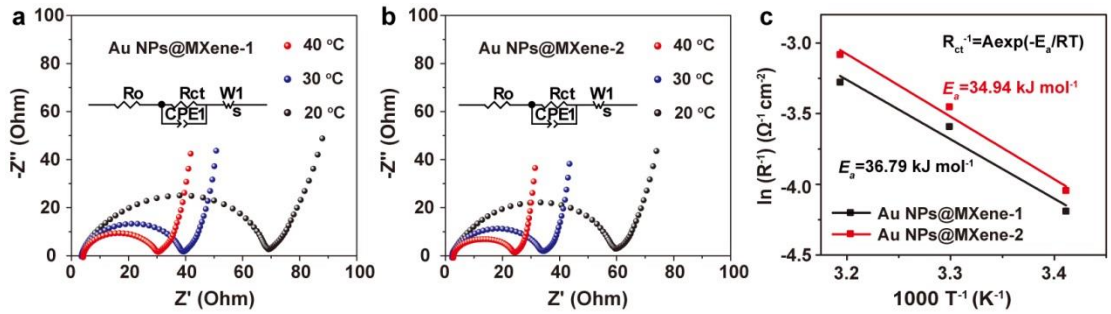

Figure S12. (a,b) EIS profiles of Li-S cells with Au NPs@MXene-1-decorated and Au NPs@MXene-2-decorated separators at different temperatures. (c) Activation energy profiles of different separators.

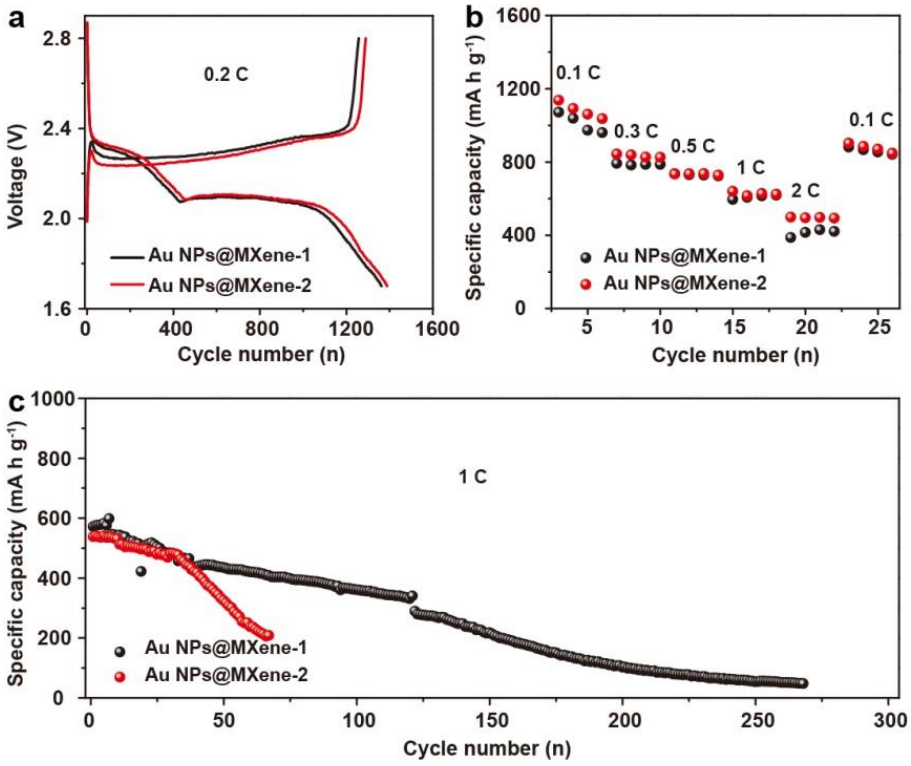

Figure S13. (a) Galvanostatic charge-discharge profiles of Li-S cells with Au NPs@MXene-1-decorated and Au NPs@MXene-2-decorated separators at 0.2 C. (b) Rate performance of S cathode with different separators. (c) Cycling performance at 1 C.

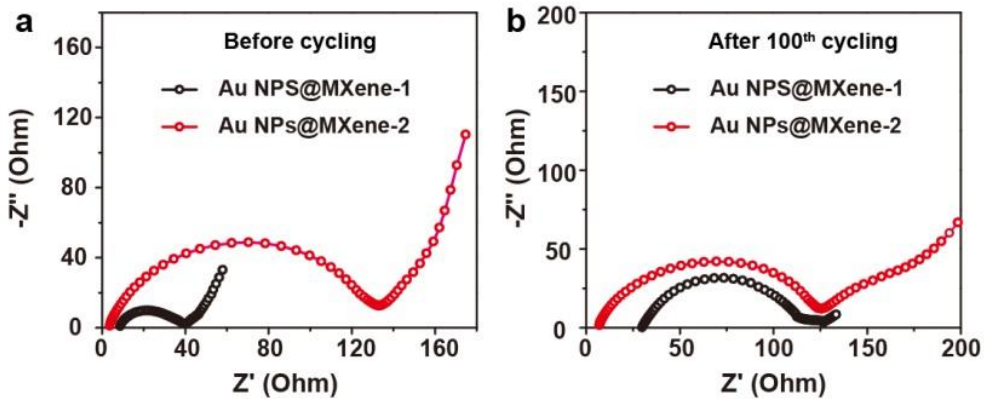

Figure S14. EIS profiles of Li-S cells with Au NPs@MXene-1-decorated separator and Au NPs@MXene-2-decorated separator (a) before and (b) after 100th cycling.

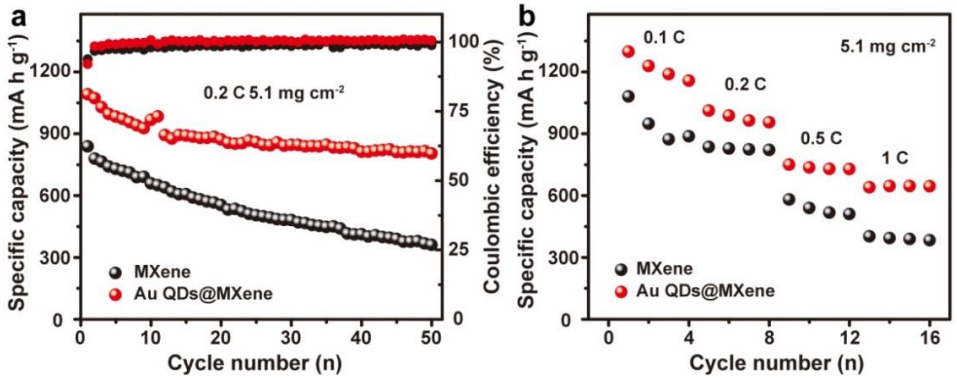

Figure S15. (a) Cycling performance at 0.2 C and (b) rate performance at different rates of the Li-S batteries with MXene-decorated and Au QDs@MXene-decorated separator with a high sulfur loading of 5.1 mg cm^{-2} (E/S ratio of 13.7 μL mg^{-1}).

Table S1. EIS data of various modified separators at different temperatures.

	T (ºC)	MXene	Au QDs@MXene (6 nm)	Au NPs@MXene-1 (11 nm)	Au NPs@MXene-2 (20 nm)
R_{ct} (Ω)	20	75.42	43.20	66.02	57.08
	30	46.26	27.52	36.28	31.58
	40	24.86	18.14	26.50	21.81